INNO-U-62

Cooling and Heating System of Shinshu University Building by Enhanced Aquifer Thermal Energy Storage

Katsuyuki Fujinawa[1], Akira Tomigashi[2]

[1] Dept. of Civil Engineering, Shinshu University, Nagano, Japan, Phone/ Fax: +81-26-269-5285,
e-mail: fujinawa@shishu-u.ac.jp

[2] Dept. of Civil Engineering, Shinshu University and Yachiyo Engineering Co., Ltd., Tokyo, Japan,
Phone: +81-3-5906-1878, Fax: +81-3-5906-0826, e-mail: tomigashi@yachiyo-eng.co.jp

1. Introduction

An enhanced aquifer thermal energy storage (E-ATES) system consisted of 5 withdrawal/injection wells and 5 monitor wells was constructed at Shinshu University, Nagano, Japan. Since November 15, 2011, a pilot plant of groundwater-source heat pump (GSHP) system coupled with the E-ATES has been put into operation for cooling and heating two lecture rooms of a building. For the sake of comparison, a conventional air-source HP (ASHP) system was also constructed for cooling and heating one lecture room of the same building. The SCOP of the GSHP system during the winter season of 2011-2012 has been improved by modification of the GSHP system and was favorably compared with that of the ASHP system.

The efficiency of the E-ATES depends on projections of cold and heat plumes in their stored aquifers, which can be facilitated by numerical simulations. Application of SWATER3dp (Subsurface Water and Thermal Energy Resources), a numerical simulation tool based on prism finite elements in three dimension, makes it possible to design an optimal operation that depends on field conditions and characteristics of facilities to be air-conditioned.

In order to identify hydrogeologic and thermal properties of the aquifer system, a variety of field tests were completed, which include all-core boring, electrical log, thermal log, pumping test, and thermal and salt-water tracer test (Tomigashi and Fujinawa, 2011). The data of the salt-water tracer tests were used to identify longitudinal dispersivity and hydraulic conductivity of aquifers by using an inversion method based on numerical solution obtained by SIFEC3dp (Salt-Water Intrusion by Finite Elements and Characteristics) (Fujinawa, et al., 2009) and Powel's optimization method (POM) (e.g., Fujinawa, 1983). Furthermore, thermal response test (TRT) was also conducted at a site close to the building to identify thermal conductivity of aquifers by using an inversion method based on the exact analytical solution and POM.

Finally, numerical simulations using SWATER3dp and the identified parameters were conducted to predict the migration of injected cold and heat plume under the condition of performed operation and future projection.

In this paper, the GSHP system with the E-ATES is briefly introduced and the achievements of this pilot project during the first winter season are presented in terms of SCOP and temperature of rooms and waters at various observation points. Furthermore, after showing the results of the inversion processes, a simulated scope of the E-ATES is presented using temperature distribution in aquifers.

2. The groundwater-source HP system

In the fiscal year of 2010, a pilot project of GSHP system coupled with E-ATES was initiated at Nagano campus of Shinshu University located in the central part of Nagano basin, Japan. The temperature of this area rises beyond 30 deg C more than 50 days a year and goes below zero about 100 days a year with accumulated snowfall of 170 cm on average. Hence, cooling during summer and heating during winter are a common practice in this area. This means that there is a great potential to conserve energy for cooling and heating by shifting from fossil fuels to a renewable thermal energy generated by ATES.

In a typical ATES system, groundwater is pumped up and waste heat from cooling process is stored in a warm aquifer zone, and vice versa. However, the stored heat or cold may be transported by flowing groundwater and dissipate due to heat conduction and dispersion unless groundwater flow and heat transport is properly handled. The basic idea of E-ATES is to establish a withdrawal/injection well system along groundwater flow path and to control groundwater flow by adjusting hydraulic gradient by means of withdrawal and injection. This system enables maximized heat and cold recovery by optimizing the withdrawal and injection rates at nested wells. Table 1 summarizes specific features of various underground thermal energy storage (UTES) systems. The E-ATES is superior to borehole thermal energy storage (BTES) and conventional ATES (C-ATES) in terms of energy output per borehole, recovery of stored thermal energy, and safety against thermal and groundwater pollution.

Table 1. Specific features of various UTES systems

Evaluation	BTES	C-ATES	E-ATES	
Energy output per borehole	×	▲	●	
Recovery of stored thermal energy	×	▲	●	
Possible Impact on geo-environment	●	×	×	× land subsidence
Safety against thermal pollution	×	×	●	× uncontrolled thermal plume
Safety against groundwater pollution	×	●	●	× leakage of antifreeze fluid
Actual performance in Japan	●	▲	—	—emerging technology
System maintenance	●	▲	▲	▲clogging of sediment pores

●excellent, ▲medium, ×poor

In order to meet the requirements of the E-ATES, 10 withdrawal, injection, and monitor wells together with one TRT borehole were constructed as shown in Figure 1. Geologic structure of the site was investigated by sampling boring core (A3) from a 75 m deep borehole and performing an electrical logging using a 80 m deep borehole (B). The lithologies and electrical logs along a well line are illustrated in Figure 2. The boring core indicates that under the surficial deposit of clay, a layer of 8 m thick, lies an unconfined aquifer of 32 m in height, which is underlain by a clay layer of 3 m thick. A confined aquifer of 21 m in height is further deposited below the clay layer. Underneath this is another clay layer of 1 m thick below which lies the third aquifer. Each aquifer, composed of sand and gravel, is named aquifer 1, 2, and 3 from the top to the bottom.

Since natural groundwater in aquifer 1 and 2 flows from NW to SE, the wells of D1 and D2 are planned to withdraw the groundwater that contains stored thermal energy while the wells of C1 and C2 are planned to be used for injecting used cool water into aquifer 1 and warm water into aquifer 2.

Figure 3 illustrates the GSHP system with the E-ATES facilitated at lecture rooms of the university building shown in Figure 1. Pumped groundwater is first treated at a pre-water treatment unit to reduce the concentration of suspended and dissolved minerals, then is sent to heat pumps connected to fan coil units (FCU) and air conditioners. After heat exchange at the heat pumps, used water is sent to a post-water treatment unit for de-aeration and finally to the injection well of C1 or C2.

The GSHP system was put into operation on November 15, 2011 for heating lecture rooms 202 and 203 while the ASHP system for lecture room 201. The first adjustment of the initial GSHP

system was the installation of an inverter to reduce electrical consumption by the pump for groundwater withdrawal from well D2 and has been implemented since December 26, 2011. The second adjustment was done to reduce the frequency of operation for de-aeration of injection water at the post-water treatment unit, which has been implemented since January 24, 2012. The third adjustment was to reuse the heat contained in the water discharged from the heat pumps. The repeated use of the waste water was done by installing a three-way valve, which went in operation after February 13, 2012.

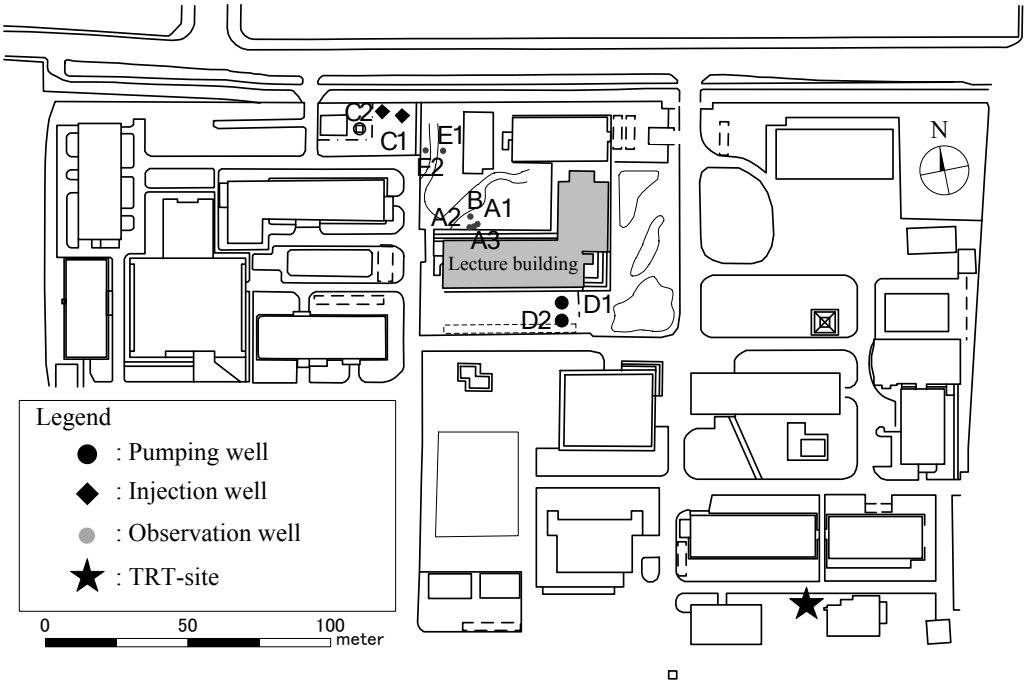

Figure 1. Well arrangement for E-ATES at Shinshu University

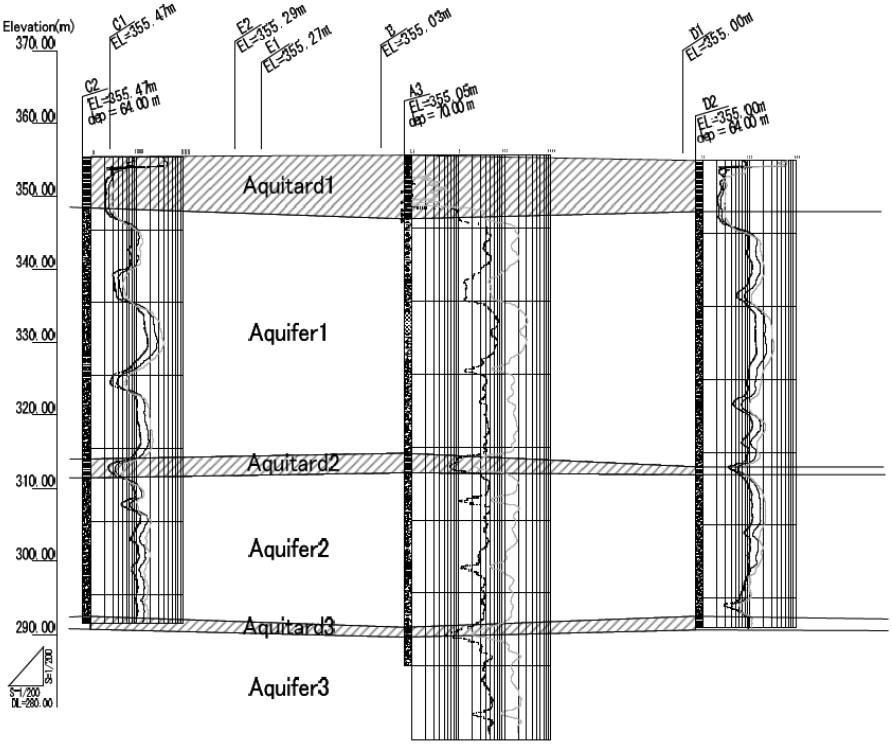

Figure 2. Lithologies with results of electrical logging at the project site

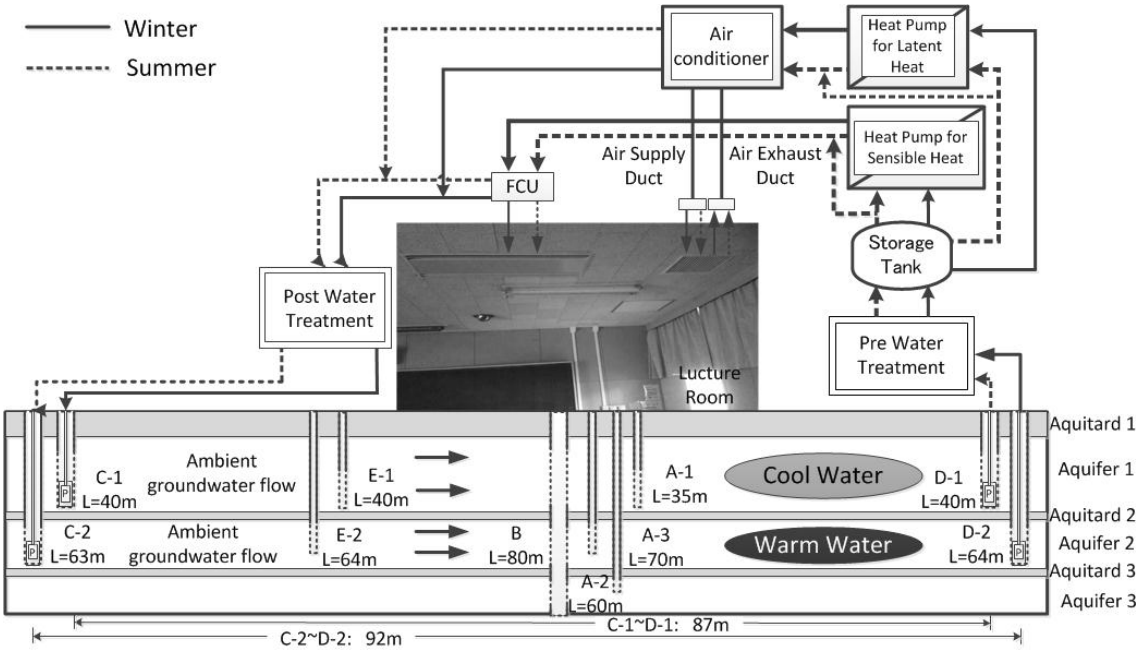

Figure 3. A schematic diagram of the groundwater-source HP system with the E-ATES

3. Results of the GSHP operation during the first winter

Figure 4 shows the changes in temperature and humidity of rooms 201 and 202. Although the set-up temperature of room 201 was 24 deg C, the achieved temperature was always significantly lower than the assigned temperature. On the contrary, the temperature of room 202 changed within an allowable range against the set-up temperature of 21.5 deg C, showing that the GSHP system gave more satisfactory result compared to the ASHP system.

Daily changes in SCOP of the GSHP and ASHP system are compared in Figure 5. It should be noted that SCOP of the GSHP system has been remarkably improved by the aforementioned adjustments of the system, and the GSHP system could finally achieve higher efficiency than the ASHP system.

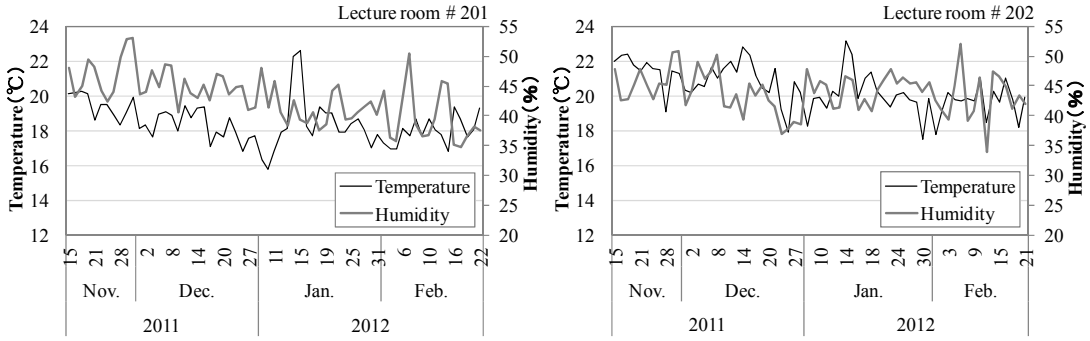

Figure 4. Temporal changes in temperature and humidity of rooms 201 and 202

Figure 6 illustrates the changes in temperature at the primary-side inlet and outlet of the heat pump for latent heat exchange on 12/21/2011, 1/16/2012, 1/25/2012, and 2/16/2012 while Figure 7 for sensible heat exchange. By comparing the data of 12/21/2011, 1/16/2012, and 1/25/2012, it is shown that the efficiency of the GSHP system was gradually improved. Furthermore, the installation of the three way valve that made it possible to reuse the water with temperature of more than 12.5 deg C discharged from the heat pumps drastically contributed to raise SCOP.

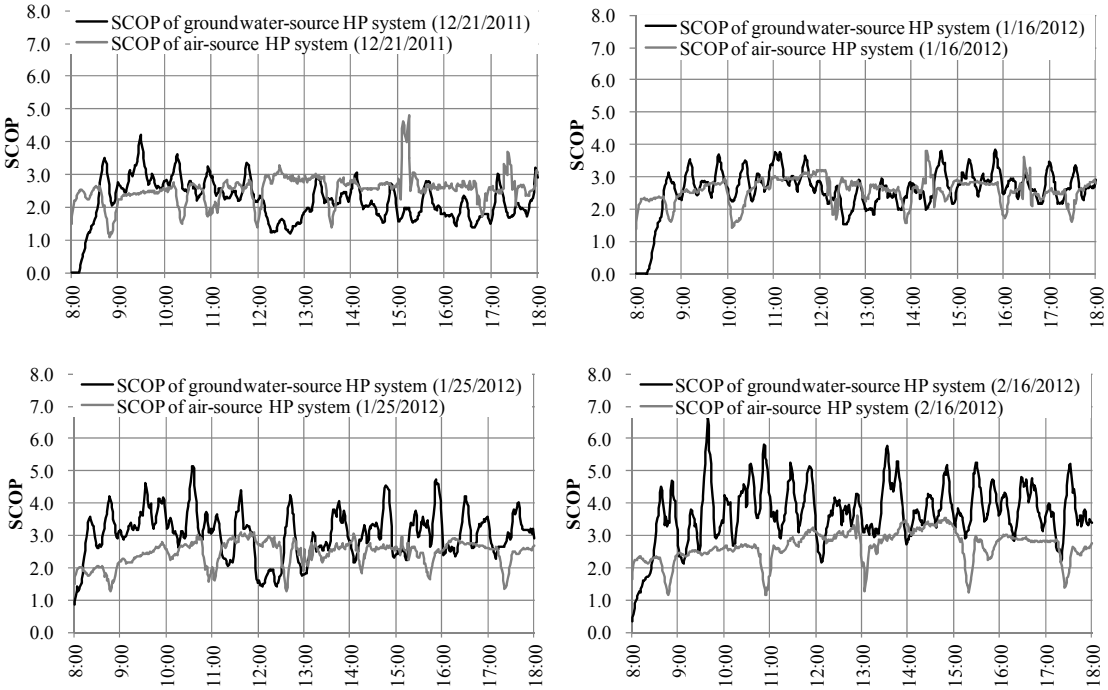

Figure 5. Comparison of SCOP changes between GSHP and ASHP system on representative days during each adjustment stage

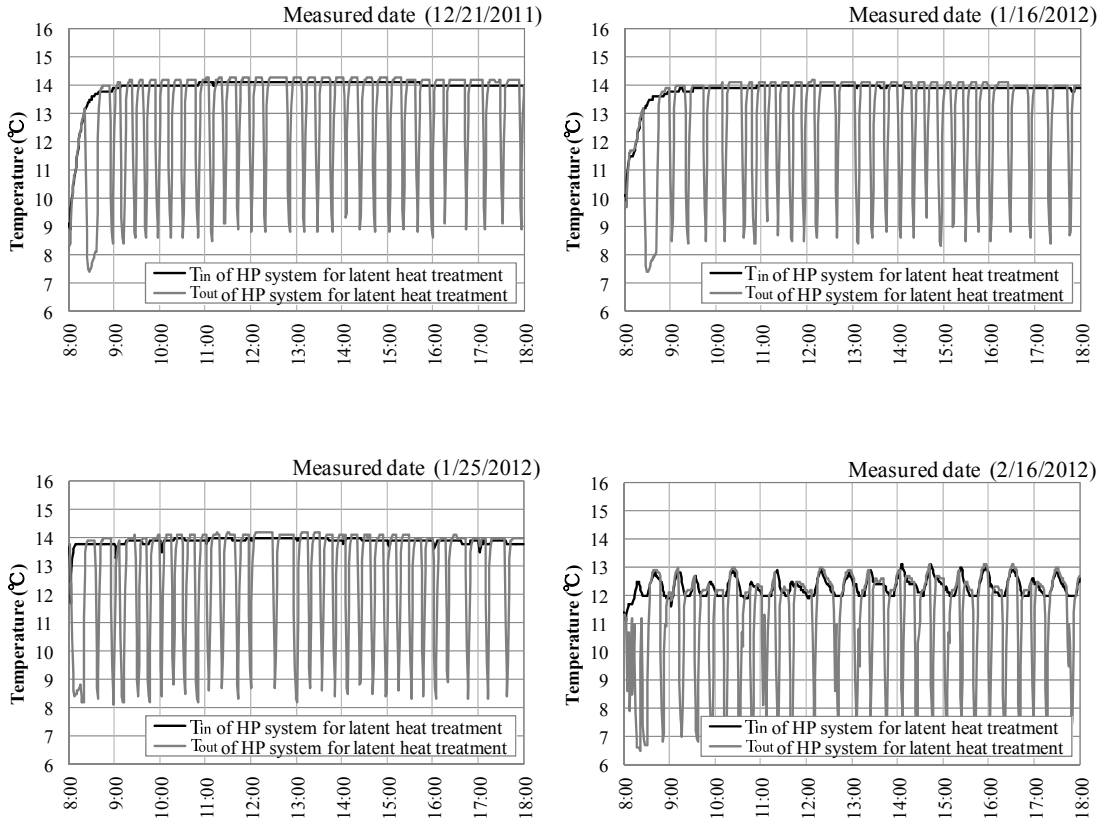

Figure 6. Temperature changes at the inlet and outlet of the heat pump for latent heat exchange on representative days during each adjustment stage

Figure 8 represents relationships between outdoor temperatures and SCOP of the GSHP and ASHP system. SCOP of the ASHP system lowers as outdoor temperature goes down. On the

contrary, SCOP of the GSHP system is raised when outdoor temperature goes down. It is also clearly shown in the figure that the each adjustment of the system contributed to improve SCOP.

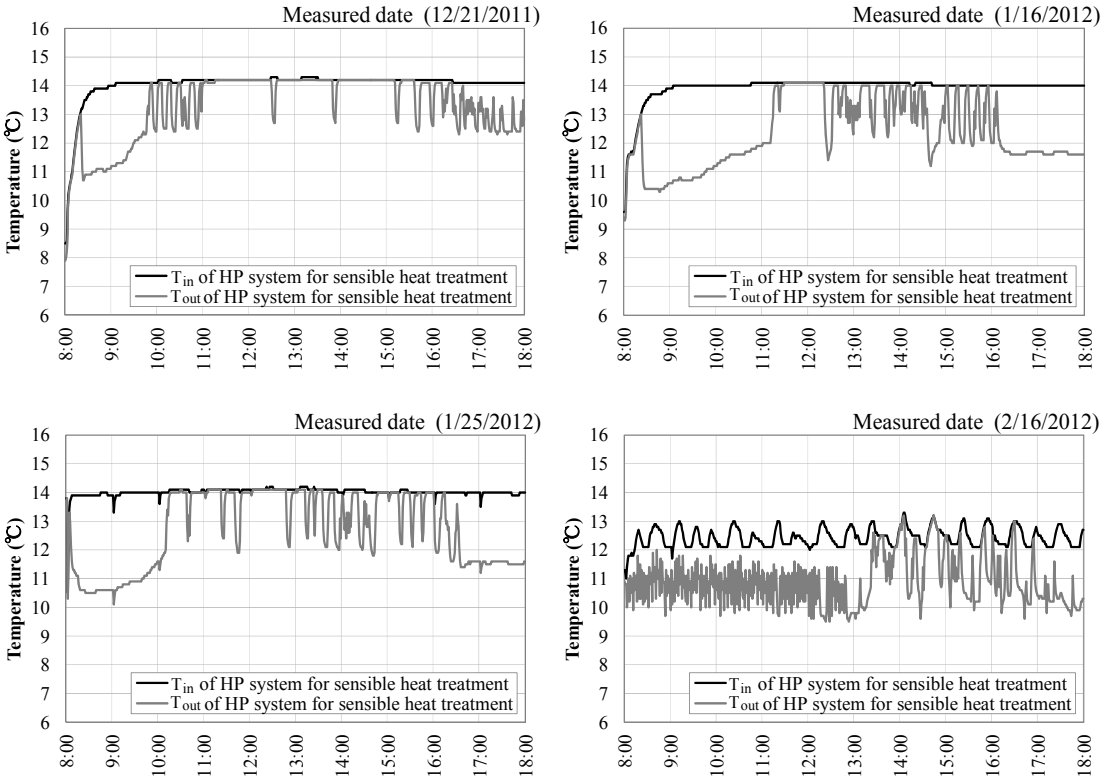

Figure 7. Temperature changes at the inlet and outlet of the heat pump for sensible heat exchange on representative days during each adjustment stage

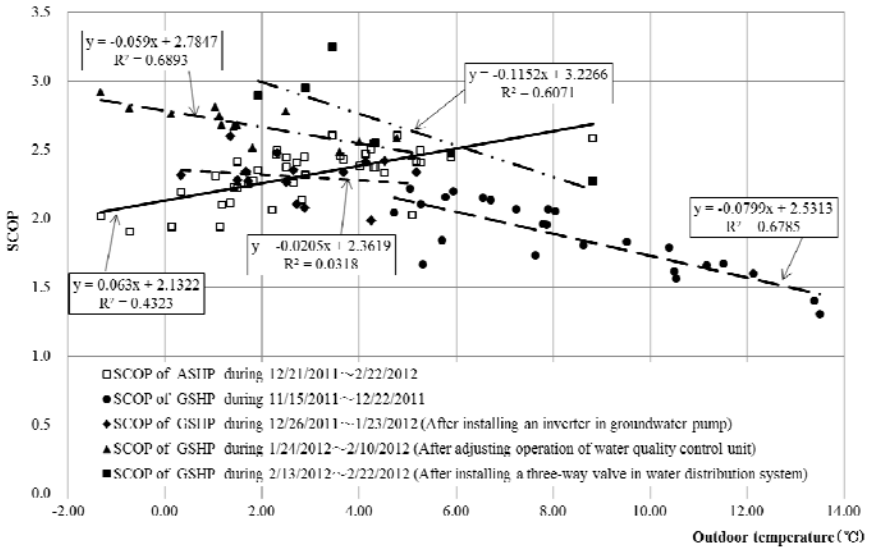

Figure 8. Relationship between outdoor temperature and SCOP of GSHP and ASHP system

4. Parameter identification for numerical simulations of heat transport in aquifers

Heat in subsurface is transported by heat conduction, thermal dispersion, and forced and natural convection asssociated with flowing groundwater. Numerical simulation tools serve as a good indicator for improving efficiency of the E-ATES. For this purpose, precise evaluation of aquifer parameters is prerequisite to assure the ulilization of simulation tools. In order to identify aquifer parameters, tracer tests using salt water were performed for each aquifer (Tomogashi and Fujinawa, 2011). Salt water in a storage tank was injected into an injection well,

and electrical conductivity and hydraulic head were observed at a monitor well 3.8m apart from the injection well. The observed data of the salt-water tracer tests were used to identify longitudinal dispersivities and hydraulic conductivities by using a newly-developed inversion method based on numerical solutions obtained by SIFEC3dp (Salt-Water Intrusion by Finite Elements and Characteristics) and Powel's optimization method (POM). These parameters are inversely identified so that the error calculated as a Euclidian norm between observed and calculated concentration vector be minimized. The theory of this inversion method is discussed elsewhere and only the results are illustrated here in Figure 9, where the identified longitudinal dispersivities for aquifer 1 and 2 were 3.56 m and 10.09m, respectively.

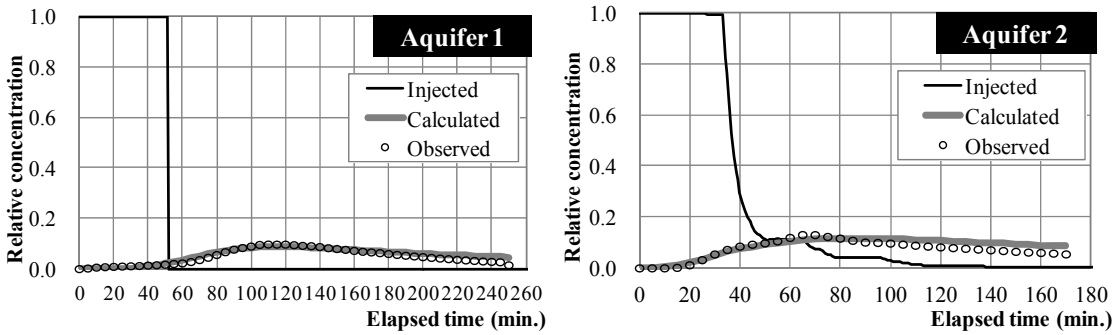

Figure 9. Changes in observed and calculated salt concentration relative to the injected for aquifer 1 and 2

It is a common practice to identify thermal conductivities of geologic formations by performing a thermal response test (TRT) and determing the slope of the average fluid temperature versus the natural log of time (Gehlin, 2002). We developed an optimization method to inversely identify thermal conductivities by minizing the error evaluated as a Euclidian norm between observed and calculated temperature vector. The inversion method is applied to an exact analytical solution to heat transport in a homogeneous medium with a line source of constant heat injection with the aid of POM, which uses all measured data in contrast to the conventional method. Figure 10 shows the result of TRT and the comparison between measured and calculated. The identified thermal conductivity at the TRT site was 2.52 W/(mK).

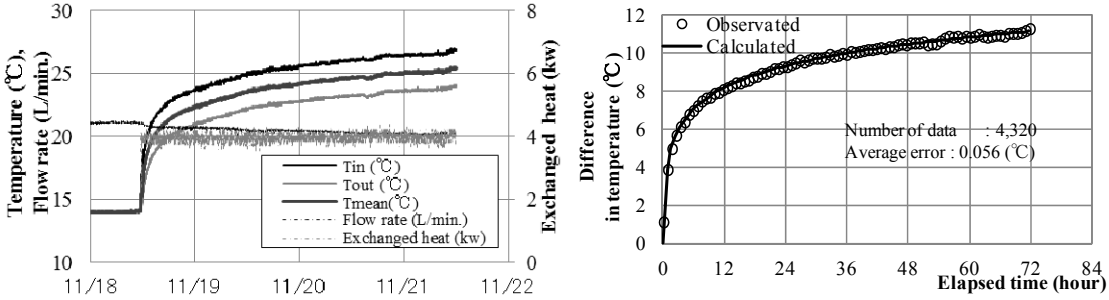

Figure 10. Results of TRT at Shinshu Univeristy campus (left) and comparison between observed and calculated (right)

5. Numerical simulation of the heat transport in aquifers affected by the GSHP system and its calculated results

In order to facilitate an optimal design of the E-ATES, a code of numerical simulation, SWATER3dp, was developed. SWATER3dp is a code to solve a set of partial differential equations for variable-density, saturated-unsaturated, coupled flow and heat transport in three dimension. The governing equations and auxiliary formulas adopted in the code are given in the appendix. Figure 11 shows the finite element mesh used to simulate groundwater flow and heat transport at the pilot project site. The number of nodes used is 25,002, and the number of elements 47,632. The dimension of the model is 200m long, 100m wide, and 64.7m deep.

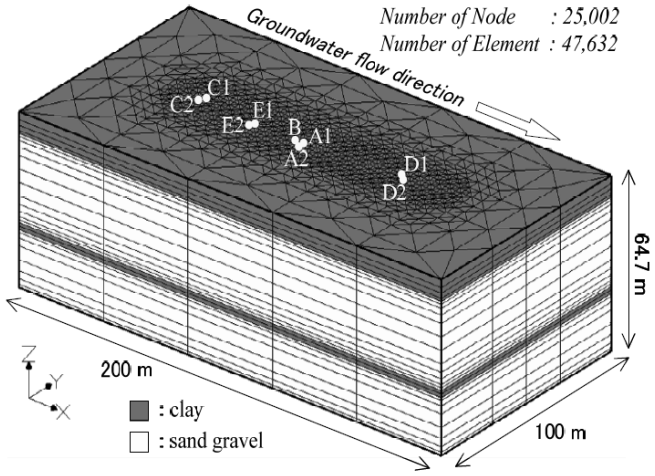

Figure 11. The finite element mesh used for the pilot project of the E-ATES at Shinshu University

Table 2 is the scenario under which the numerical simulation was performed while Table 3 shows hydrogeological and thermal parameters adopted in the simulation. These parameters are noted in the appendix along with the governing equations.

Table 2. Conditions of operation for the GSHP system

Operation mode	Period		Pumping/Injection rate	Injection water temperature	Condiotion for simulation
	date	number of days	(m^3/hour)		
Heating	11/15～2/14	93	8.3～11.0 / 9.1～11.5	12.0～13.9	performed
Heating	2/15～3/31	44	10.5	9.0deg C	projected
Suspend	4/1～5/31	61	-	-	
Cooling	6/1～9/30	122	10.5	19.0deg C	
Suspend	10/1～10/31	31	-	-	

Table 3. Parameters used for the numerical simulation

Saturated hydraulic conductivity at a reference temperature of 4deg C			
Clay	K_r	0.00036	m/hr
Sand gravel (Aquifer 1)	K_r	0.306	m/hr
Sand gravel (Aquifer 2)	K_r	1.104	m/hr
Porosity	ε	0.200	-
Saturated water content	θ_s	0.200	-
Residual water content	θ_r	0.100	-
Parameter of van Genuchten eq.			
α		5.270	/m
β		2.138	-
Longitudinal dispersivity (Aquifer 1)	α_L	3.561	m
Longitudinal dispersivity (Aquifer 2)	α_L	10.089	m
Transverse dispersivity (Aquifer 1)	α_T	0.3561	m
Transverse dispersivity (Aquifer 2)	α_T	1.0089	m
Volumetric heat capacity of			
Solid phase	$(\rho C)_s$	550.00	J/m3K
Water phase	$(\rho C)_w$	1161.11	J/m3K
Air phase	$(\rho C)_a$	0.3361	J/m3K
Heat conductivity of			
Solid phase	λ_s	5.252	W/mK
Water phase	λ_w	0.594	W/mK
Air phase	λ_a	0.024	W/mK

Figure 12 shows the seasonal changes in the temperature distribution in vertical and horizontal plane as simulated under the operation scenario listed in Table 2. The optimized control of groundwater flow can be achieved by withdraw-injection operation of the wells. In order to seek the best operational scenario so that the possible transport of cold and heat stored in aquifer systems be controlled to maximize its recovery, the other numerical simulations are being performed at the moment under various scenarios. These results will be presented at the conference.

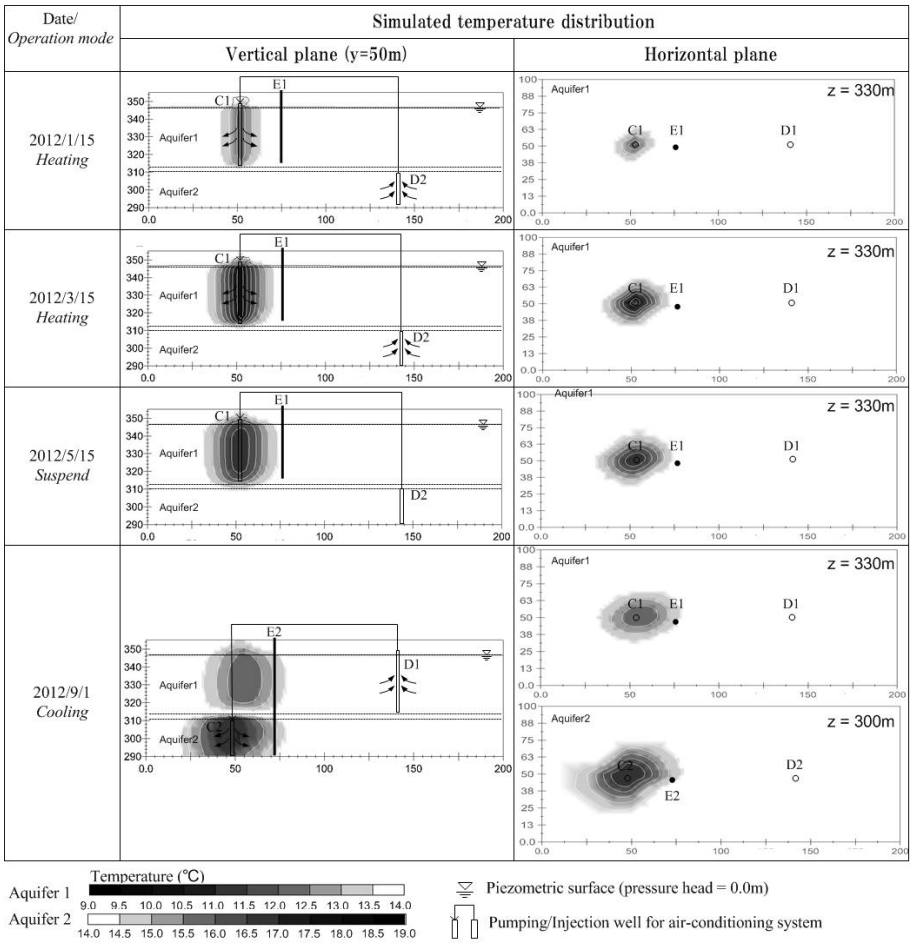

Figure 12. Simulated results of groundwater temperature profile

6. Conclusions

This paper deals with three research topics related to ATES. Firstly, a pilot plant of GSHP system coupled with E-ATES that controls groundwater flow to maximize the use of stored heat was constructed and operated during the winter of 2011-2012. The achieved SCOP of the system was compared with that of a conventional ASHP system and the proposed system showed a superior performance to the ASHP. Secondly, two inversion methods for identifying hydrogeologic and thermal parameters of aquifers were developed. Dispersivities and hydraulic conductivities were identified by conducting salt-water tracer tests and using a Powel's optimization method incorporated with SIFEC3dp (Salt-Water Intrusion by Finite Elements and Characteristics). The thermal conductivity of aquifers was also inversely identified by conducting thermal response tests and using a Powel's optimization method incorporated with an exact analytical solution to the heat conduction in aquifers. The application of these inversion methods gave satisfactory results. Finally, a numerical simulation code, SWATER3dp (Subsurface Water and Thermal Energy Resources), was run to simulate heat transport in the project in order to optimize the operation scenario of the E-ATES, and its results are presented.

7. Acknowledgements

This project has been financially supported by Japanese New Energy and Industrial Technology Development Organization. Planning, constructing, and running this GSHP system with the E-ATES and proving the efficiency of the system have been carried out by a cooperative team joined by H.Momota, M.Suzuki, K.Morino, K.Okamura, and K.Yoneyama of Simizu Co. Ltd.,

N.Takagi at Architecture Dept. of Shinshu University, and T.Ishihara and K.Uehara, undergraduate students of Shinshu University. We are grateful for their works done with us.

8. References

[1] Tomigashi, A., K. Fujinawa: Enhanced aquifer thermal energy storage for cooling and heating of Shinshu University building using a nested well system, Sustainable Development and Planning V, pp.871-882, 2011.
[2] Fujinawa, K., T. Iba, Y. Fujihara and T. Watanabe : Modeling interaction of fluid and salt in an aquifer/lagoon systems, Ground Water, Vol.47, No.1, pp.35-48, 2009.
[3] Fujinawa, K.: Asymptotic solutions to the convection-dispersion equation and Powell's optimization method for evaluating groundwater velocity and dispersion coefficients from observed data of single dilution tests, Journal of Hydrology, 62, 1983.
[4] Gehlin, S.: Thermal Response Test, Doctoral Thesis, Luea University, 2002.

9. Appendix

The governing equation for flow of water in saturated-unsaturated zone is given by

$$\nabla \bullet \{\frac{\mu_r K_r}{\mu}(\nabla h_r + \frac{\rho}{\rho_r}\nabla z)\} - \sum_{i=1}^{n_q} Q_i \delta_i = \rho(S_e S_s \frac{\partial h_r}{\partial t} + C_s \frac{\partial h_r}{\partial t}) + \varepsilon S_e \frac{\partial \rho}{\partial t} \qquad (1)$$

where ρ and ρ_r are the density of water; μ and μ_r are the dynamic viscosity of freshwater; S_e is the fractional effective water saturation; S_s is the specific storage; h_r is the pressure head in terms of water of a reference temperature; $C_s (= \varepsilon \partial S_e / \partial h_r)$ is the soil water capacity; ε is the fractional porosity; K_r is the hydraulic conductivity in terms of water of a reference temperature; Q_i is the withdrawal rate of a pumping well i; δ_i is the Dirac delta function for the pumping or injection well; z is the upward vertical coordinate. For unsaturated porous media, van Genuchten provided functional relations for the parameters S_e and K_r in Equation (1) as follows:

$$S_e = \frac{\theta - \theta_r}{\theta_s - \theta_r} = \frac{1}{(1 + |\alpha h_f|^{\beta})^r}, \quad (\gamma = 1 - \frac{1}{\beta}) \quad (2), \qquad K_r = K_{rs} S_e^{1/2} \left\{1 - \left(1 - S_e^{1/\gamma}\right)^{\gamma}\right\}^2 \qquad (3)$$

where θ, θ_s and θ_r are the volumetric water content (VWC), the saturated VWC, and the residual VWC, respectively; α and β are the characteristic constants of soil to be evaluated from experiments; K_{rs} is the saturated hydraulic conductivity in terms of a reference temperature.

The governing equation for heat transport in the saturated-unsaturated zone is given by

$$\nabla \bullet (\boldsymbol{\lambda} \nabla T) - \theta (\rho C)_w \nabla \bullet (\mathbf{v} T) = (\rho C) \frac{\partial T}{\partial t} \qquad (4)$$

Where T is temperature; $(\rho C)_w$ is the volumetric heat capacity of water phase. Assigning $(\rho C)_s$ of the volumetric heat capacity of solid phase and $(\rho C)_a$ of the volumetric heat capacity of air phase, the bulk volumetric heat capacity (ρC) is calculated by

$$(\rho C) = \varepsilon S (\rho C)_w + \varepsilon (1 - S)(\rho C)_a + (1 - \varepsilon)(\rho C)_s \qquad (5)$$

The tensor element of $\boldsymbol{\lambda}$ is given by

$$\lambda_{ij} = \lambda_{ed} + (\lambda_{md})_{ij} = (\rho C) D_{ij} \qquad (6)$$

where λ_{ed} and λ_{md} are the bulk thermal conductivity and the mechanical thermal dispersivity; D_{ij} is the hydrodynamic dispersion coefficient. And the dispersion tensor is defined by

$$D_{ij} = \alpha_{ijkm} |v_k \| v_m| / |v| + \kappa_e$$
$$\alpha_{ijkm} = \alpha_T \delta_{ij} \delta_{km} + (\alpha_L - \alpha_T)(\delta_{ik} \delta_{jm} + \delta_{im} \delta_{jk}) / 2 \qquad (7)$$

where v is the average velocity; v_k and v_m are the velocity components of two coordinate directions, k and m; δ_{ij} is the Kronecker Delta; κ_e is the bulk thermal diffusivity; α_L is the longitudinal dispersivity; α_T is the transverse dispersivity.